Anisotropic short-range structure of $Co_{0.16}Pd_{0.84}$ alloy films having perpendicular magnetic anisotropy

Sang-Koog Kim
Advanced Light Source, Lawrence Berkeley National Laboratory, University of California, Berkeley, California 94720

V. A. Chernov
Siberian Synchrotron Radiation Center of Budker Institute of Nuclear Physics, Institute of Catalysis, 630090 Novosibirsk, Russia

J. B. Kortright
Materials Science Division, Lawrence Berkeley National Laboratory, University of California, Berkeley, California 94720

Y. M. Koo
Department of Materials Science and Engineering, Pohang University of Science and Technology, Pohang 790-784, Republic of Korea

Polarized Co K edge extended x-ray absorption fine structure measurements obtained with electric vector parallel and perpendicular to the film plane indicate differences in Co bonding along these two directions in room-temperature evaporated $Co_{0.16}Pd_{0.84}$ alloy films. A local modulation of the Co fraction whose amplitudes are 0.05–0.09 exists along the growth direction in the alloy films. Pd underlayer and Pd spacer layers alternated with the alloy layer induce coherency strains resulting in an anisotropic effective strain state. Both anisotropic strain and local compositional modulation are likely to contribute to the perpendicular magnetic anisotropy observed in these alloys. © *1997 American Institute of Physics.* [S0003-6951(97)02225-0]

Because of their potential application in magneto-optical high-density recording, Co/Pd and Co/Pt multilayer films exhibiting perpendicular magnetic anisotropy (PMA) have been extensively studied to understand the anisotropy mechanism over the last decade.[1–5] Co–Pd and Co–Pt alloy films were since found to exhibit PMA, and relationships between alloy composition, preparation conditions, microstructure, and magnetic properties have been established.[6–11] Weller *et al.*[7,9] reported that Co–Pt and Co–Pd alloys have PMA, 100% remanence, and high coercivity comparable to those in their multilayer systems.

Previous studies of the alloy films have provided differing suggestions and mostly indirect evidence relating PMA to microstructure. A polarized extended x-ray absorption fine structure (EXAFS) study of Co–Pt alloy films concludes its origin is likely to be clustering (ordering) of Co atoms in surface normal (111) planes yielding internal interfaces[12] based on a model of intermixing at the interface of superlattice.[4] As for the Co–Pd alloy, the origin of its PMA was speculated to be a similar compositional anisotropy of Co atoms in the Pd matrix[10] without direct evidence. The origin of PMA in the alloys has remained unclear because of limited direct structural information and lack of theoretical study while the PMA in multilayers has been explained by the interfacial, magnetocrystalline, and magnetoelastic anisotropy (MEA) originating from the uniaxial asymmetry.[1–4]

To investigate the short range structure of Co–Pd alloy films, we analyzed polarized EXAFS's which provide direct short range information about the average Co environment. Polarized EXAFS was chosen because of its ability to provide both directional- and chemical-specific nearest-neighbor information around Co absorbers.[13] Our results demonstrate that Co–Co correlations are different between parallel (∥)

and perpendicular (⊥) to the surface of the Co–Pd alloy films.

Four room-temperature coevaporated alloy samples were studied, one grown directly onto a Si wafer ($Co_{0.16}Pd_{0.84}$), two with Pd underlayers [$Co_{0.16}Pd_{0.84}$/Pd(100 Å), $Co_{0.16}Pd_{0.84}$/Pd(200 Å)], remaining one alternated by Pd spacer, [Pd(50 Å)/$Co_{0.16}Pd_{0.84}$(50 Å)]×10. All samples have PMA as confirmed by rectangular perpendicular magnetic hysteresis loops measured by vibrating sample magnetometer shown in Fig. 1. All hysteresis loops show that the easy axis of magnetization is oriented out-of-plane. X-ray diffraction shows all samples have (111)-textured polycrystalline structure, with (111)-peak positions corresponding to Co composition within 1% difference from those by EXAFS analysis. Atomic force microscopy shows the samples have small surface roughnesses of 4–6 Å and lateral correlation lengths of 300–400 Å. Thus, roughness-induced PMA via a surface dipole-dipole interaction[14] is not expected.

Polarized Co K-edge EXAFS's were measured as a fluorescence yield for each sample by orienting the electric field vector **E** nearly perpendicular ($E_\perp$) and exactly parallel ($E_\parallel$) to the film surface at near-grazing incidence.[15] Because of the 111 texture of the films, in the $E_\perp$ polarization only atoms out of the plane with respect to Co absorbers contribute to the EXAFS signals, while in the $E_\parallel$ polarization backscattering from atoms both in and out of the film plane contributes. From this knowledge, we can resolve directional information of the short range structure surrounding Co absorbers. In our case, the first nearest neighbors are resolved by analyzing the first shell around Co emitters.

Anisotropy in Co–Co correlation is seen directly in the background-subtracted, normalized EXAFS's of $E_\parallel$ and $E_\perp$ polarization, as seen in Fig. 2 for the simple alloy film. A
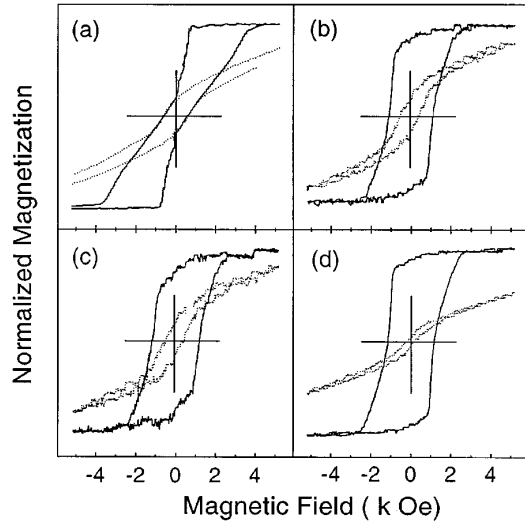
FIG. 1. Normalized magnetic hysteresis loops of $Co_{0.16}Pd_{0.84}$ alloy films with different structural parameters: without Pd underlayer in (a), with 100 Å thick Pd underlayer in (b) and 200 Å thick Pd underlayer in (c), and alternated by Pd spacer $[Co_{0.16}Pd_{0.84}(50 Å)/Pd(50 Å)]\times 10$ in (d). Solid and dotted lines indicate applied field directions perpendicular and parallel to the film plane, respectively.

FIG. 3. Radial distribution functions extracted from Fourier transform of EXAFS. The best-fit data (solid lines) are compared with the experimental ones (circles). The radial coordinate does not correspond to the actual inter-atomic distance, as phase function for the central scattering atoms has not been included. Dotted and dashed lines indicate the out-of-plane and in-plane atoms of both Co and Pd, respectively. The apparent discrepancy between total amplitude and sum of each elements amplitude results because the FT function of EXAFS is complex.

difference in peak-to-peak amplitude is clearly seen in the first period of EXAFS oscillation with a small phase difference due to contributions of different bonding lengths at higher k. These differences indicate structural anisotropy. By Fourier transforms (FT) of EXAFS functions $k^3\chi(k)$ (k is the photoelectron momentum), radial distribution functions (RDFs) of Co emitters (circles) are obtained as in Fig. 3. A split first peak containing Co–Co and Co–Pd contributions are seen.

To separate Co and Pd contributions and obtain detailed structure, we fitted EXAFS data assuming these two back-scatters described by theoretical amplitudes and phases generated by FEFF6.[16] Including two peaks within a range of $R =[1.3-3.4 Å]$, data were fitted in real space according to a novel method of simultaneous fitting[17,18] with both RDF's Fourier transformed in a range $k=[2.8-9.7 Å^{-1}]$ taken in the $E_\perp$ and $E_\parallel$ polarization. The variable parameters include N coordination number, R radial distance, and σ^2 structural disorder in R for both Co and Pd backscatters which vary in
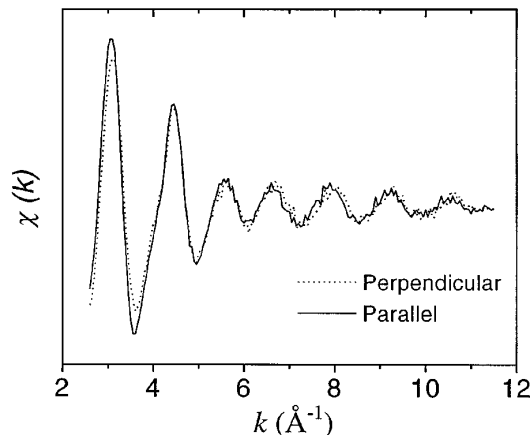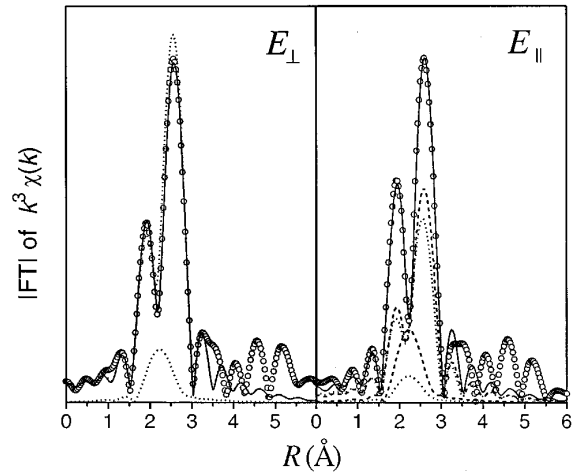

FIG. 2. Fluorescence-yield Co K-edge EXAFS's of $Co_{0.16}Pd_{0.84}$ alloy film which are background subtracted and then normalized by an edge step near inflection point from absorption spectra taken in two geometries with E perpendicular and parallel to the film plane.

the fit with a constraint of 12 surrounding atoms in the first shell.

The spectra taken with the $E_\parallel$ polarization are fitted using the variable parameters for the out-of-plane atoms *simultaneously* fitted in the $E_\perp$ polarization to obtain the structural parameters of the in-plane atoms. The best-fit curves (solid lines) and experimental data (open circles) are shown in Fig. 3 together with each contribution from Co and Pd neighbors of the in-plane (dashed lines) and out-of-plane (dotted lines) as previously mentioned. The resulting parameters are shown in Table I. Comparison of N and R between the in-plane and out-of-plane atoms reveals structural anisotropy.

To understand the origin of anisotropy in Co–Co first neighbors, we extend the notion of clustering or ordering anisotropy with a simple analytic model which assumes that locally alternating 111 planes parallel to the film surface have a high (x_h) and low (x_l) fraction of Co. The ratio of average Co coordination number ($\bar{N}_{Co}$) to the Pd one ($\bar{N}_{Pd}$) for both in- and out-of-plane atoms can be expressed as

$$\frac{\bar{N}_{Co}^{out}}{\bar{N}_{Pd}^{out}} = \frac{2x_h x_l}{x_h(1-x_l)+x_l(1-x_h)}, \tag{1}$$

$$\frac{\bar{N}_{Co}^{in}}{\bar{N}_{Pd}^{in}} = \frac{x_h x_h + x_l x_l}{x_h(1-x_h)+x_l(1-x_l)}. \tag{2}$$

Using Eqs. (1) and (2) with $\bar{N}_{Co}$ from Table I and $\bar{N}_{Pd}=6 -\bar{N}_{Co}$, the x_l and x_h are determined as in Table I. Unequal values of x_h and x_l indicate a short range ordering normal to the surface of the Co–Pd alloy films, which does not exist in equilibrium phase. The determined amplitudes of the local modulation of the Co fraction defined by $(x_h-x_l)/2$ are 0.05–0.09 for all the alloys as shown in Table II. A decrease to 0.05 is likely to be an increase in the roughness of the interface between the Pd underlayer and the alloy layer. We refer to the local modulation of the Co fraction as short-range composition-modulation (SRCM) to compare with

TABLE I. Best-fit parameters from simultaneous fitting. Determined local Co fractions, x_h and x_l, and Co strains parallel and perpendicular to the film plane. $(x_h - x_l)/2$ is amplitude of local modulation, and $(\bar{\epsilon}_\parallel - \epsilon_\perp)/2$ is effective strain anisotropy. $\bar{x}$ stands for average Co composition which is defined by $(x_h + x_l)/2$.

	$Co_{0.16}Pd_{0.84}$	$Co_{0.16}Pd_{0.84}/Pd(100\ \text{Å})$	$Co_{0.16}Pd_{0.84}/Pd(200\ \text{Å})$	$[Co_{0.16}Pd_{0.84}(50\ \text{Å})/$ $Pd(50\ \text{Å})]\times10$
$\bar{N}_{Co}^{in}$	1.26 ± 0.31	1.02 ± 0.22	1.06 ± 0.21	1.2 ± 0.29
$\bar{N}_{Co}^{out}$	0.62 ± 0.21	0.81 ± 0.24	0.84 ± 0.16	0.7 ± 0.29
$\bar{R}_{Co}^{in}$	2.612 ± 0.025	2.651 ± 0.017	2.658 ± 0.016	2.63 ± 0.021
$\bar{R}_{Co}^{out}$	2.611 ± 0.034	2.606 ± 0.025	2.597 ± 0.016	2.57 ± 0.031
$\sigma_{Co}^{in2}=\sigma_{Co}^{out2}$	0.0082 ± 0.0016	0.0067 ± 0.00055	0.0070 ± 0.00057	0.0090 ± 0.00086
$\bar{x}$	0.157 ± 0.0078	0.152 ± 0.0076	0.158 ± 0.0079	0.157 ± 0.0078
x_h	0.248	0.205	0.21	0.236
x_l	0.0649	0.10	0.104	0.0775
$\bar{\epsilon}_\parallel$	0.0424	0.058	0.061	0.048
$\bar{\epsilon}_\perp$	0.0415	0.034	0.028	0.017
$(x_h - x_l)/2$	0.0916	0.053	0.054	0.079
$(\bar{\epsilon}_\parallel - \bar{\epsilon}_\perp)/2$	0.0005	0.012	0.016	0.015

long-range composition modulation (LRCM) in the case of a multilayer system. For all alloy films, the SRCM is present even though its amplitude is smaller than that for a perfect superlattice. It was found that the multilayer with a LRCM has the smaller amplitude of the LRCM by diffuse interfaces than that expected or desired in preparation.[15]

The anisotropic Co–Co distances determined for EXAFS analysis can be interpreted as an effective anisotropic strain compared to bulk Co. Average strains of Co parallel ($\parallel$) and perpendicular ($\perp$) to the film plane can be derived from cylindrical symmetry of our (111) textured geometry,

$$\bar{\epsilon}_\parallel = \bar{R}_{Co}^{in}/R - 1 , \qquad (3)$$

$$\bar{\epsilon}_\perp = 2\bar{R}_{Co}^{out}\sin\theta/(R\sqrt{3}) - 1 , \qquad (4)$$

where $\theta = \arccos(\bar{R}_{Co}^{in}/2\bar{R}_{Co}^{out})$, and R is the Co–Co nearest distance of 2.506 Å for fcc bulk Co. $\bar{\epsilon}_\perp$ as well as $\bar{\epsilon}_\parallel$ values are tensile as seen in Table I. Tensile Co–Co distances compared to bulk are expected since Co is in a unit cell dominated by Pd. In the Pd matrix, Co atoms have an effective strain anisotropy by $\pm(\bar{\epsilon}_\parallel - \bar{\epsilon}_\perp)/2$, the positive and negative signs stand for the directions parallel and perpendicular to the film plane, respectively. The alloy without Pd underlayers has a negligible strain anisotropy, but the remaining alloys have an evident strain anisotropy of ±0.012, ±0.016, and ±0.015. Interfaces in the samples having Pd under and spacer layers explain why only these samples exhibit this anisotropic effective strain. The interplay between the coherent elastic and incoherent interfacial energy may affect the magnitude of the effective strain.

As seen in Fig. 1, the shapes of hysteresis loops confirm the link between PMA and a short range structure discussed above. Both the SRCM and the anisotropy in Co–Co distances appear to play a role in the PMA of these samples. Increasing effective strain anisotropy through Pd under and spacer layers leads to better perpendicular magnetic hysteresis loops. Among the samples studied the best quality magnetic hysteresis curve is observed for the sample $[Co_{0.16}Pd_{0.84}(50\ \text{Å})/Pd(50\ \text{Å})]\times10$, which can be expected by the anisotropic strain and the amplitude of SRCM as shown in Table I.

Finally, we conclude that the origin of PMA in the Co–Pd alloy samples studied here is due to the structural origins of both chemical ordering similar to broken symmetry in multilayer system and anisotropic strain. These macroscopic effects are closely consistent with the microscopic origins of electronic hybridization of Co atoms near Pd neighbors or Pt ones and its strain dependence proposed in theory by Kyuno et al.[3]

[1] P. F. Carcia, A. D. Meinhaldt, and A. Suna, Appl. Phys. Lett. **47**, 178 (1985).
[2] G. H. O. Daalderop, P. J. Kelly, and M. F. H. Schuurmans, Phys. Rev. B **42**, 7270 (1990).
[3] K. Kyuno, J.-G. Ha, and R. Yamamoto, Phys. Rev. B **54**, 1092 (1996).
[4] J. M. MacLaren and R. H. Victora, J. Appl. Phys. **76**, 6069 (1994).
[5] M. H. Kryder, J. Appl. Phys. **57**, 3913 (1985).
[6] S. Tsunashima, N. Nagase, K. Nakamura, and S. Uchiyama, IEEE Trans. Magn. **25**, 3761 (1989).
[7] D. Weller, H. Brändle, and C. Chappert, J. Magn. Magn. Mater. **121**, 461 (1993).
[8] C.-J. Lin and G. L. Gorman, Appl. Phys. Lett. **61**, 1600 (1992).
[9] D. Weller, H. Brändle, G. Gorman, C.-J. Lin, and H. Notarys, Appl. Phys. Lett. **61**, 2726 (1992).
[10] J. R. Childress, J. L. Duvail, S. Jasmin, A. Barthélémy, A. Fert, A. Schuhl, O. Durand, and P. Galtier, J. Appl. Phys. **75**, 6412 (1994).
[11] S. Shiomi, H. Okazawa, T. Nakakita, T. Kobayashi, and M. Masuda, Jpn. J. Appl. Phys. 1 **32**, L315 (1993).
[12] T. A. Tyson, S. D. Conradson, R. F. C. Farrow, and B. A. Jones, Phys. Rev. B **54**, R3702 (1996).
[13] V. G. Harris, K. D. Aylesworth, B. N. Das, W. T. Elam, and N. C. Koon, Phys. Rev. Lett. **69**, 1939 (1992).
[14] P. Bruno, J. Appl. Phys. **64**, 3153 (1988).
[15] S. K. Kim, Y. M. Koo, V. A. Chernov, and H. Padmore, Phys. Rev. B **53**, 11114 (1996); S. K. Kim, Y. M. Koo, and V. A. Chernov, J. de Physique IV (1997) (to be published).
[16] M. Newville, Ph.D. thesis, Washington University, 1995.
[17] J. J. Rehr, J. M. Deleon, S. I. Zabinsky, and R. C. Albers, J. Am. Chem. Soc. **113**, 5135 (1991).
[18] E. A. Stern, M. Newville, B. Ravel, Y. Yacoby, and D. Haskel, Physica B **209**, 117 (1995).